1.7 Ternary Equilibrium

Since most commercial alloys are based on at least three components, an understanding of ternary phase diagrams is of great practical importance. The ideas that have been developed for binary systems can be extended to systems with three or more components[4].

The composition of a ternary alloy can be indicated on an equilateral triangle (the Gibbs triangle) whose corners represent 100% A, B or C as shown in Fig. 1.40. The triangle is usually divided by equidistant lines parallel to the sides marking 10% intervals in atomic or weight per cent. All points on lines parallel to BC contain the same percentage of A, the lines parallel to AC represent constant B concentration, and lines parallel to AB constant C concentrations. Alloys on PQ for example contain 60% A, on RS 30% B, and TU 10% C. Clearly the total percentage must sum to 100%, or expressed as mole fractions

$$X_A + X_B + X_C = 1 \tag{1.62}$$

The Gibbs free energy of any phase can now be represented by a vertical distance from the point in the Gibbs triangle. If this is done for all possible compositions the points trace out the free energy *surfaces* for all the possible phases, as shown in Fig. 1.41a. The chemical potentials of A, B and C in any phase are then given by the points where the *tangential plane* to the free energy surfaces intersects the A, B and C axes. Figure 1.41a is drawn for a

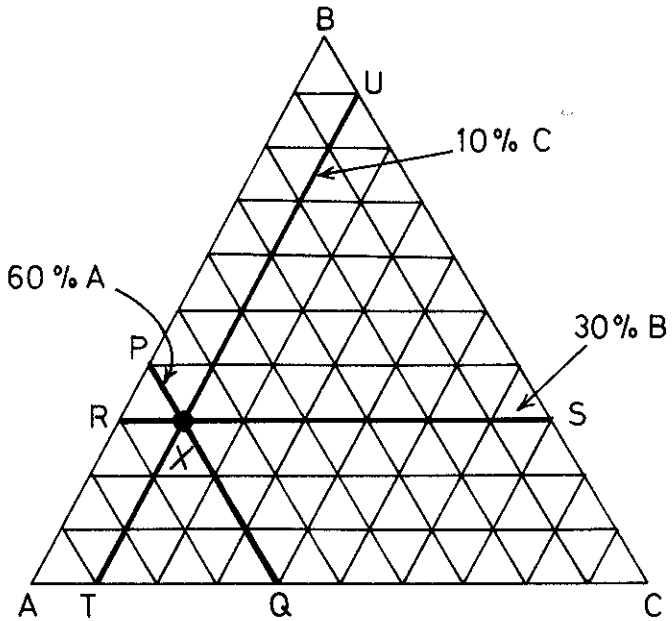

Fig. 1.40 The Gibbs triangle.

system in which the three binary systems AB, BC and CA are simple eutectics. Free energy surfaces exist for three solid phases α, β and γ and the liquid phase, L. At this temperature the liquid phase is most stable for all alloy compositions. At lower temperatures the G^L surface moves upwards and eventually intersects the G^α surface as shown in Fig. 1.41b. Alloys with compositions in the vicinity of the intersection of the two curves consist of α + L at equilibrium. In order for the chemical potentials to be equal in both

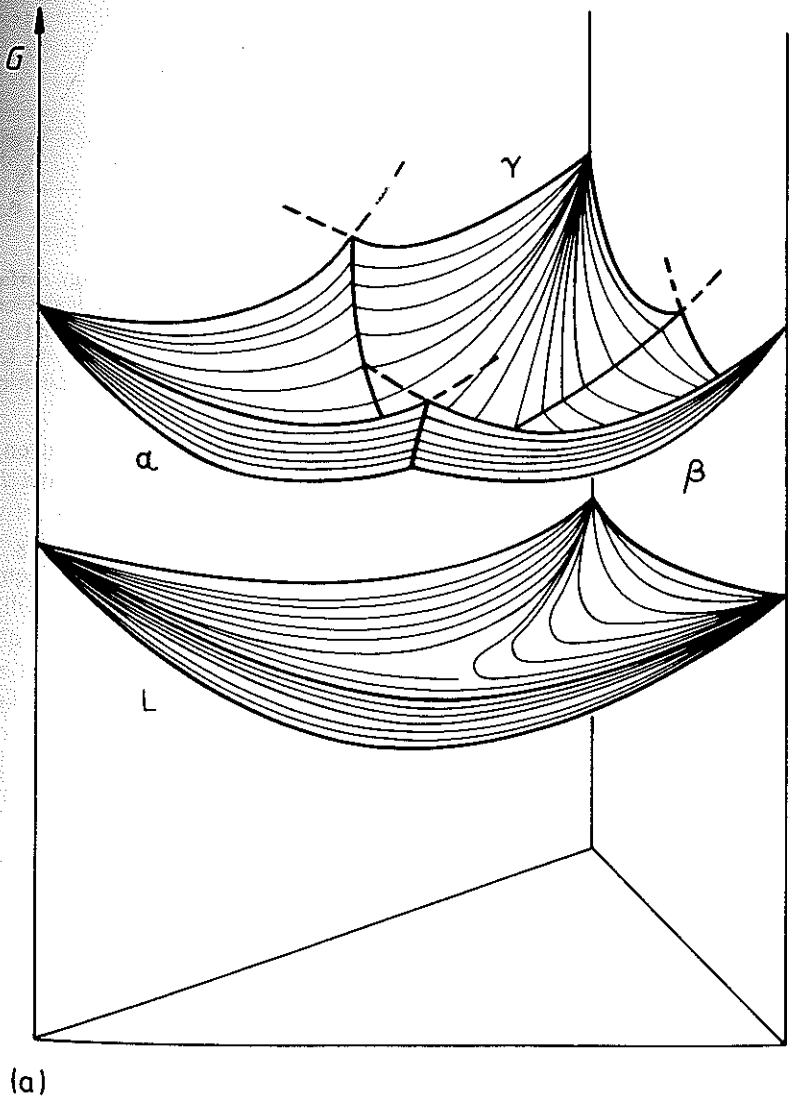

Fig. 1.41 (a) Free energies of a liquid and three solid phases of a ternary system.

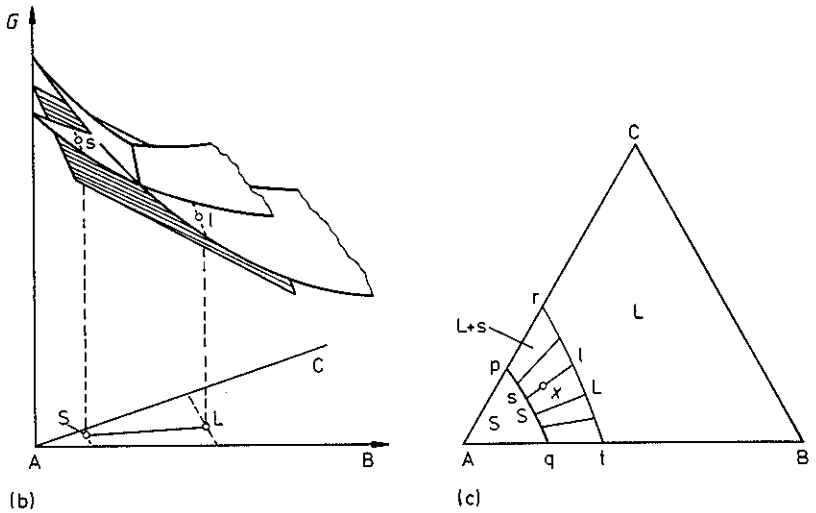

Fig. 1.41 (*Cont.*) (b) A tangential plane construction to the free energy surfaces defines equilibrium between s and l in the ternary system. (c) Isothermal section through a ternary phase diagram obtained in this way with a two-phase region (L+S) and various tie-lines. The amounts of l and s at point x are determined by the lever rule. (After P. Haasen, *Physical Metallurgy*, Cambridge University Press, Cambridge, 1978.)

phases the compositions of the two phases in equilibrium must be given by points connected by a *common tangential plane*, for example s and l in Fig. 1.41b. These points can be marked on an *isothermal section* of the equilibrium phase diagram as shown in Fig. 1.41c. The lines joining the compositions in equilibrium are known as *tie-lines*. By rolling the tangential plane over the two free energy surfaces a whole series of tie-lines will be generated, such as pr and qt, and the region covered by these tie-lines pqtr is a two-phase region on the phase diagram. An alloy with composition x in Fig. 1.41c will therefore minimize its free energy by separating into solid α with composition s and liquid with composition l. The relative amounts of α and L are simply given by the lever rule. Alloys with compositions within Apq will be a homogeneous α phase at this temperature, whereas alloys within BCrt will be liquid.

On further cooling the free energy surface for the liquid will rise through the other free energy surfaces producing the sequence of isothermal sections shown in Fig. 1.42. In Fig. 1.42f, for example, the liquid is stable near the centre of the diagram whereas at the corners the α, β and γ solid phases are stable. In between are several two-phase regions containing bundles of tie-lines. In addition there are three-phase regions known as *tie-triangles*. The L + α + β triangle for example arises because the common tangential plane simultaneously touches the G^{α}, G^{β} and G^{L} surfaces. Therefore any alloy with a composition within the L + α + β triangle at this temperature will be in equilibrium as a three-phase mixture with compositions given by the corners

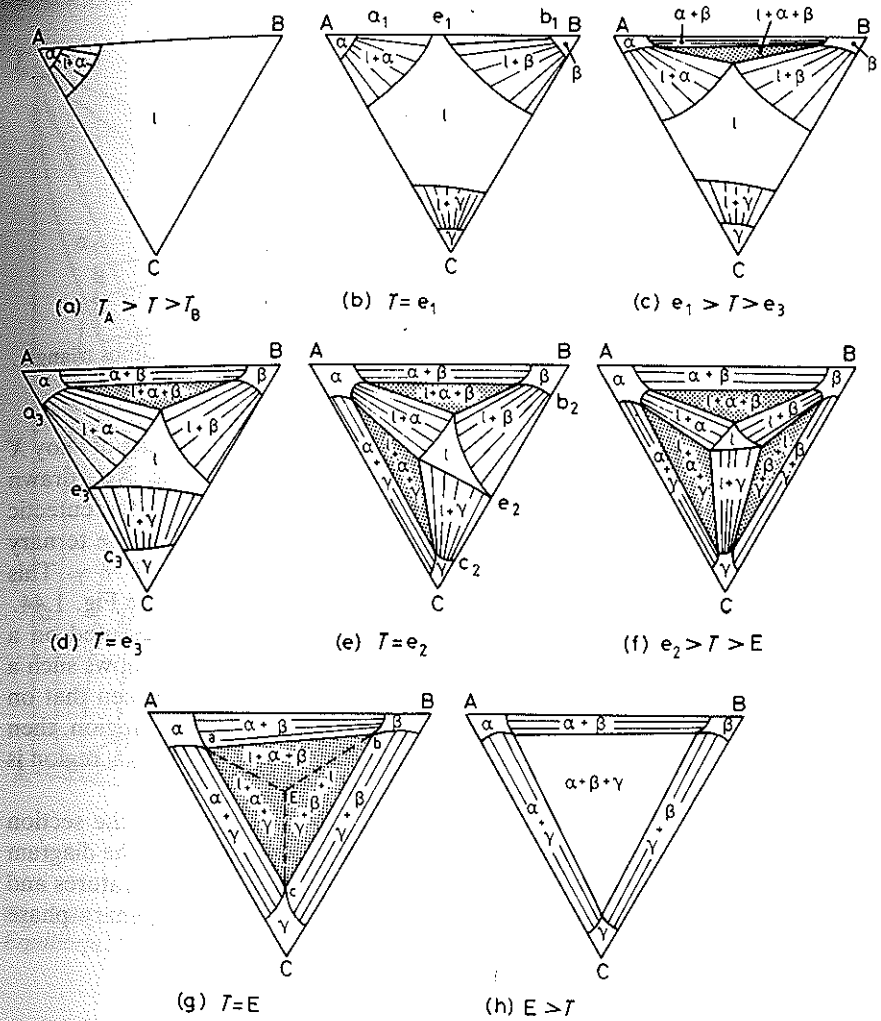

Fig. 1.42 Isothermal sections through Fig. 1.44. (After A. Prince, *Alloy Phase Equilibria*, Elsevier, Amsterdam, 1966.)

of the triangle. If the temperature is lowered still further the L region shrinks to a point at which four phases are in equilibrium L + α + β + γ. This is known as the ternary eutectic point and the temperature at which it occurs is the ternary eutectic temperature, Fig. 1.42g. Below this temperature the liquid is no longer stable and an isothermal section contains three two-phase regions and one three-phase tie triangle α + β + γ as shown in Fig. 1.42h. If isothermal sections are constructed for all temperatures they can be combined into a three-dimensional ternary phase diagram as shown in Fig. 1.44.

In order to follow the course of solidification of a ternary alloy, assuming equilibrium is maintained at all temperatures, it is useful to plot the liquidus

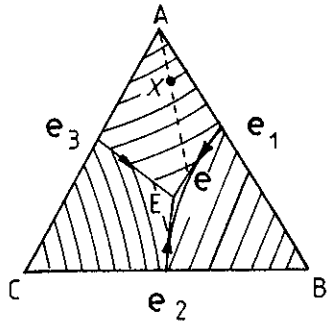

Fig. 1.43 A projection of the liquidus surfaces of Fig. 1.44 onto the Gibbs triangle.

surface contours as shown in Fig. 1.43. During equilibrium freezing of alloy X the liquid composition moves approximately along the line Xe (drawn through A and X) as primary α phase is solidified; then along the eutectic valley eE as both α and β solidify simultaneously. Finally at E, the ternary eutectic point, the liquid transforms simultaneously into $\alpha + \beta + \gamma$. This sequence of events is also illustrated in the perspective drawing in Fig. 1.44.

The phases that form during solidification can also be represented on a *vertical section* through the ternary phase diagram. Figure 1.45 shows such a section taken through X parallel to AB in Fig. 1.44. It can be seen that on cooling from the liquid phase the alloy first passes into the L + α region, then into L + α + β, and finally all liquid disappears and the $\alpha + \beta + \gamma$ region is entered, in agreement with the above.

An important limitation of vertical sections is that in general the section will not coincide with the tie-lines in the two-phase regions and so the diagram only shows the phases that exist in equilibrium at different temperatures and *not* their compositions. Therefore they can not be used like binary phase diagrams, despite the superficial resemblance.

1.8 Additional Thermodynamic Relationships for Binary Solutions

It is often of interest to be able to calculate the change in chemical potential ($d\mu$) that results from a change in alloy composition (dX). Considering Fig. 1.46 and comparing triangles it can be seen that

$$-\frac{d\mu_A}{X_B} = \frac{d\mu_B}{X_A} = \frac{d(\mu_B - \mu_A)}{1} \tag{1.63}$$

and that the slope of the free energy–composition curve is given by

$$\frac{dG}{dX_B} = \frac{\mu_B - \mu_A}{1} \tag{1.64}$$

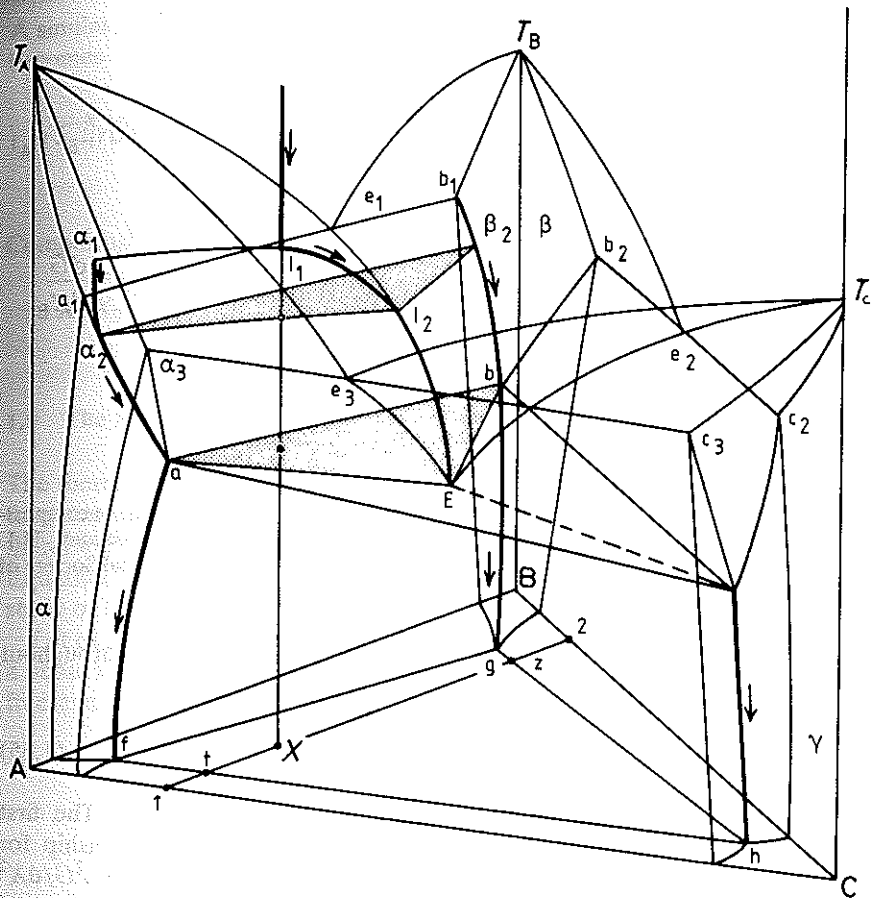

Fig. 1.44 The equilibrium solification of alloy X. (After A. Prince, *Alloy Phase Equilibria*, Elsevier, Amsterdam, 1966.)

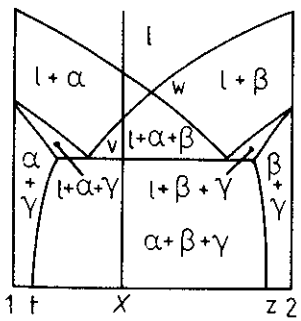

Fig. 1.45 A vertical section between points 1, 2 and X in Fig. 1.44. (After A. Prince, *Alloy Phase Equilibria*, Elsevier, Amsterdam, 1966.)

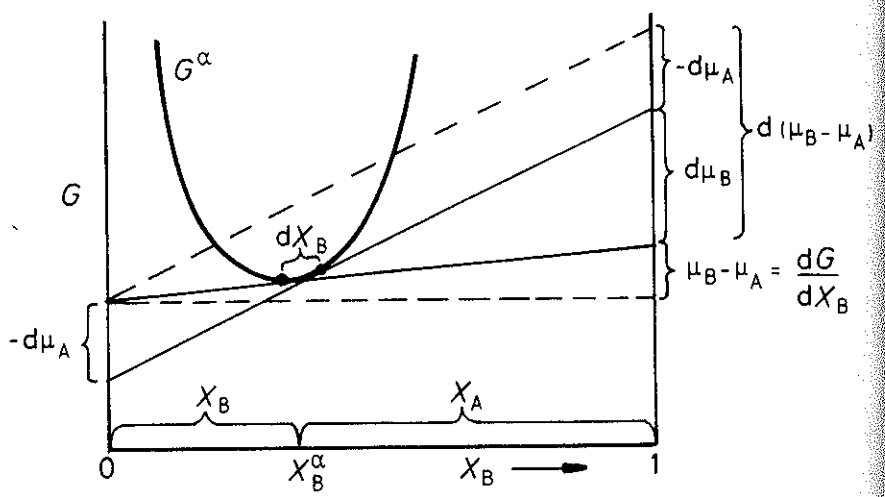

Fig. 1.46 Evaluation of the change in chemical potential due to a change in composition. (After M. Hillert, in *Lectures on the Theory of Phase Transformations*, H.I. Aaronson (Ed.), ©The American Society for Metals and The Metallurgical Society of AIME, New York, 1969.)

Substituting this expression into Equation 1.63 and multiplying throughout by $X_A X_B$ leads to the following equalities:

$$-X_A d\mu_A = X_B d\mu_B = X_A X_B \frac{d^2G}{dX^2} dX_B \tag{1.65}$$

which are the required equations relating $d\mu_A$, $d\mu_B$ and dX_B. The first equality in this equation is known as the Gibbs-Duhem relationship for a binary solution. Note that the B subscript has been dropped from d^2G/dX^2 as $d^2G/dX_B^2 \equiv d^2G/dX_A^2$. For a regular solution differentiation of Equation 1.39 gives

$$\frac{d^2G}{dX^2} = \frac{RT}{X_A X_B} - 2\Omega \tag{1.66}$$

For an ideal solution $\Omega = 0$ and

$$\frac{d^2G}{dX^2} = \frac{RT}{X_A X_B} \tag{1.67}$$

Equation 1.65 can be written in a slightly different form by making use of activity coefficients. Combining Equations 1.41 and 1.43 gives

$$\mu_B = G_B + RT \ln \gamma_B X_B \tag{1.68}$$

Therefore

$$\frac{d\mu_B}{dX_B} = \frac{RT}{X_B}\left\{1 + \frac{X_B}{\gamma_B}\frac{d\gamma_B}{dX_B}\right\} = \frac{RT}{X_B}\left\{1 + \frac{d \ln \gamma_B}{d \ln X_B}\right\} \tag{1.69}$$

A similar relationship can be derived for $d\mu_A/dX_B$. Equation 1.65 therefore becomes

$$-X_A d\mu_A = X_B d\mu_B = RT\left\{1 + \frac{d \ln \gamma_A}{d \ln X_A}\right\} dX_B = RT\left\{1 + \frac{d \ln \gamma_B}{d \ln X_B}\right\} dX_B \tag{1.70}$$

Comparing Equations 1.65 and 1.70 gives

$$X_A X_B \frac{d^2G}{dX^2} = RT\left\{1 + \frac{d \ln \gamma_A}{d \ln X_A}\right\} = RT\left\{1 + \frac{d \ln \gamma_B}{d \ln X_B}\right\} \tag{1.71}$$

1.9 The Kinetics of Phase Transformations

The thermodynamic functions that have been described in this chapter apply to systems that are in stable or metastable equilibrium. Thermodynamics can therefore be used to calculate the driving force for a transformation, Equation 1.4, but it cannot say how fast a transformation will proceed. The study of how fast processes occur belongs to the science of *kinetics*.

Let us redraw Fig. 1.1 for the free energy of a single atom as it takes part in a phase transformation from an initially metastable state into a state of lower free energy, Fig. 1.47. If G_1 and G_2 are the free energies of the initial and

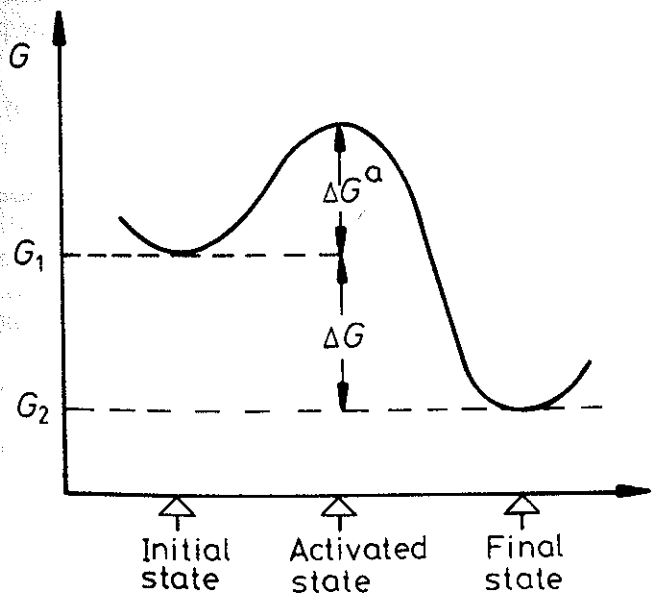

Fig. 1.47 Transformations from initial to final state through an activated state of higher free energy.

final states, the driving force for the transformation will be $\Delta G = G_2 - G_1$. However, before the free energy of the atom can decrease from G_1 to G_2 the atom must pass through a so-called *transition* or *activated* state with a free energy ΔG^a above G_1. The energies shown in Fig. 1.47 are average energies associated with large numbers of atoms. As a result of the random thermal motion of the atoms the energy of any particular atom will vary with time and occasionally it may be sufficient for the atom to reach the activated state. This process is known as *thermal activation*.

According to kinetic theory, the probability of an atom reaching the activated state is given by $\exp(-\Delta G^a/kT)$ where k is Boltzmann's constant (R/N_a) and ΔG^a is known as the *activation free energy barrier*. The rate at which a transformation occurs will depend on the frequency with which atoms reach the activated state. Therefore we can write

$$\text{rate} \propto \exp\left(-\frac{\Delta G^a}{kT}\right)$$

Putting $\Delta G^a = \Delta H^a - T\Delta S^a$ and changing from atomic to molar quantities enables this equation to be written as

$$\text{rate} \propto \exp\left(-\frac{\Delta H^a}{RT}\right) \tag{1.72}$$

This equation was first derived empirically from the observed temperature dependence of the rate of chemical reactions and is known as the *Arrhenius rate equation*. It is also found to apply to a wide range of processes and transformations in metals and alloys, the simplest of these is the process of diffusion which is discussed in Chapter 2.

References

1. See D.R. Gaskell, *Introduction to Metallurgical Thermodynamics*, p. 342, McGraw-Hill, 1973.
2. For a more detailed treatment of the structures of solid solutions, intermetallic compounds and intermediate phases see, for example, Chapters 4 and 5 in *Physical Metallurgy*, R.W. Cahn (Ed.), North-Holland, 1974 (second edition).
3. For a treatment of nonspherical precipitates see M. Ferrante and R.D. Doherty, *Acta Metallurgica*, **27**: (1979) 1603.
4. See, for example, M. Hillert, *Phase Transformations*, American Society for Metals, Ohio, 1970, Chapter 5.

Further Reading

A.H. Cottrell, *An Introduction to Metallurgy*, Chapter 14 'Alloys' and Chapter 15. 'The phase diagram', Edward Arnold, London, 1967.

D.R. Gaskell, *Introduction to Metallurgical Thermodynamics*, McGraw-Hill, New York, 1973.

P. Gordon, *Principles of Phase Diagrams in Materials Systems*, McGraw-Hill, New York, 1968.

M. Hillert, 'Calculation of Phase Equilibria', Chapter 5 in *Phase Transformations*, American Society for Metals, Ohio, 1970.

M. Hillert, 'The uses of the Gibbs free energy-composition diagrams', Chapter 1 in *Lectures on the Theory of Phase Transformations*, H.I. Aaronson (Ed.) published by the The Metallurgical Society of AIME, New York, 1975.

A. Prince, *Alloy Phase Equilibria*, Elsevier, London, 1966.

G.V. Raynor, 'Phase diagrams and their determination', Chapter 7 in R.W. Cahn (Ed.) *Physical Metallurgy*, North-Holland, 1970.

F.N. Rhines, *Phase Diagrams in Metallurgy*, McGraw-Hill, New York, 1956.

P.G. Shewmon, 'Metallurgical thermodynamics', Chapter 6 in R.W. Cahn and P. Haasen (Eds.) *Physical Metallurgy*, North-Holland, 1983.

A.D. Pelton, 'Phase diagrams', Chapter 7 in R.W. Cahn and P. Haasen (Eds.) *Physical Metallurgy*, North-Holland, 1983.

R.A. Swalin, *Thermodynamics of Solids*, Wiley, New York, second edition, 1972.

D.R.F. West, *Ternary Equilibrium Diagrams*, Chapman & Hall, 2nd edition, 1982.

C.H.P. Lupis, *Chemical Thermodynamics of Materials*, North Holland, 1983.

Exercises

1.1 The specific heat of solid copper above 300 K is given by

$$C_p = 22.64 + 6.28 \times 10^{-3} T \quad \text{J mol}^{-1}\,\text{K}^{-1}$$

By how much does the entropy of copper increase on heating from 300 to 1358 K?

1.2 With the aid of Equation 1.11 and Fig. 1.5, draw schematic free energy-pressure curves for pure Fe at 1600, 800, 500 and 300 °C.

1.3 Estimate the change in the equilibrium melting point of copper caused by a change of pressure of 10 kbar. The molar volume of copper is 8.0×10^{-6} m^3 for the liquid, and 7.6×10^{-6} for the solid phase. The latent heat of fusion of copper is 13.05 kJ mol^{-1}. The melting point is 1085 °C.

1.4 For a single component system, why do the allotropes stable at high temperatures have higher enthalpies than allotropes stable at low temperatures, e.g. H(γ-Fe) > H(α-Fe)?

1.5 Determine, by drawing, the number of distinguishable ways of arranging two black balls and two white balls in a square array. Check your answer with Equation 1.24.

1.6 By using Equations 1.30 and 1.31, show that the chemical potentials of A and B can be obtained by extrapolating the tangent to the G–X curve to $X_A = 0$ and $X_B = 0$.

1.7 Derive Equation 1.40 from 1.31 and 1.39.

1.8 15 g of gold and 25 g of silver are mixed to form a single-phase ideal solid solution.
(a) How many moles of solution are there?
(b) What are the mole fractions of gold and silver?
(c) What is the molar entropy of mixing?
(d) What is the *total* entropy of mixing?
(e) What is the molar free energy change at 500 °C?
(f) What are the chemical potentials of Au and Ag at 500 °C taking the free energies of pure Au and Ag as zero?
(g) By how much will the free energy of the solution change at 500 °C if one Au atom is added? Express your answer in eV/atom.

1.9 In the Fe–C system Fe_3C is only a metastable phase, whilst graphite is the most stable carbon-rich phase. By drawing schematic free energy–composition diagrams show how the Fe–graphite phase diagram compares to the Fe–Fe_3C phase diagram from 0 to 2 wt% Fe. Check your answer with the published phase diagram in the *Metals Handbook* for example.

1.10 Consider a multicomponent system A, B, C . . . containing several phases α, β, γ . . . at equilibrium. If a small quantity of A (dn_Amol) is taken from the α phase and added to the β phase at constant T and P what are the changes in the free energies of the α and β phases, dG^α and dG^β? Since the overall mass and composition of the system is unchanged by the above process the total free energy change $dG = dG^\alpha + dG^\beta = 0$. Show, therefore, that $\mu_A^\alpha = \mu_A^\beta$. Repeating for other pairs of phases and other components gives the general equilibrium conditions, Equation 1.48.

1.11 For aluminium $\Delta H_v = 0.8$ eV atom^{-1} and $\Delta S_v/R = 2$. Calculate the equilibrium vacancy concentration at 660 °C (T_m) and 25 °C.

1.12 The solid solubility of silicon in aluminium is 1.25 atomic % at 550 °C and 0.46 atomic % at 450 °C. What solubility would you expect at 200 °C? Check your answer by reference to the published phase diagram.

1.13 The metals A and B form an ideal liquid solution but are almost immiscible in the solid state. The entropy of fusion of both A and B is 8.4 J mol^{-1}K^{-1} and the melting temperatures are 1500 and 1300 K respectively. Assuming that the specific heats of the solid and liquid are identical calculate the eutectic composition and temperature in the A–B phase diagram.

1.14 Write down an equation that shows by how much the molar free energy of solid Cu is increased when it is present as a small sphere of radius r in liquid Cu. By how much must liquid Cu be cooled below T_m before a solid particle of Cu can grow if the particle *diameter* is (i) 2 μm, (ii) 2 nm (20 Å)? (Cu: T_m = 1085 °C = 1358 K. Atomic weight 63.5. Density 8900 kg m^{-3}. Solid/liquid interfacial energy γ = 0.144 J m^{-2}. Latent heat of melting L = 13 300 J mol^{-1}.)

1.15 Suppose a ternary alloy containing 40 atomic % A, 20 atomic % B, 40 atomic % C solidifies through a ternary eutectic reaction to a mixture of α, β and γ with the following compositions: 80 atomic % A, 5 atomic % B, 15 atomic % C; 70 atomic % B, 10 atomic % A, 20 atomic % C; and 20 atomic % B, 10 atomic % A, 70 atomic % C. What will be the mole fractions of α, β and γ in the microstructure?

1.16 Show that a general expression for the chemical potential of a component in solution is given by

$$\mu_A = G_A^0 + S_A(T_0 - T) + RT \ln \gamma_A X_A + (P - P_0)V_m$$

where G_A^0 is the free energy of pure A at temperature T_0 and pressure P_0, S_A is the entropy of A, R is the gas constant, γ_A the activity coefficient for A, X_A the mole fraction in solution, V_m is the molar volume which is assumed to be constant. Under what conditions is the above equation valid?